Supporting Information

Location-selective Growth of Two-dimensional Metallic/Semiconducting Transition Metal Dichalcogenide Heterostructures

Xue Gong[a,b,c], Xiaoxu Zhao[d], Mei Er Pam[c], Huizhen Yao[a,b], Zibo Li[a,b], Dechao Geng[c], Stephen J. Pennycook[d], Yumeng Shi*[a,b], Hui Ying Yang*[c]*

[a] International Collaborative Laboratory of 2D Materials for Optoelectronic Science & Technology of Ministry of Education, College of Optoelectronic Engineering, Shenzhen University, Shenzhen 518060, China.

[b] Engineering Technology Research Center for 2D Material Information Function Devices and Systems of Guangdong Province, College of Optoelectronic Engineering, Shenzhen University, Shenzhen 518060, China.

[c] Pillar of Engineering Product Development, Singapore University of Technology and Design, 8 Somapah Road, 487371, Singapore.

[d] Department of Materials Science and Engineering, National University of Singapore, 9 Engineering Drive 1, 117575, Singapore.

E-mail: yanghuiying@sutd.edu.sg, yumeng.shi@szu.edu.cn

Materials and Instruments

Unless otherwise noted, all chemicals were purchased from Sigma-Aldrich and used without further purification. Optical images were obtained using an Olympus BX51 microscope. AFM images were obtained using a Bruker Dimension FastScan atomic force microscope in the tapping mode. Raman spectra and PL spectra were recorded at room temperature using a WITec Raman microscope with laser excitation at 532 nm. Atomic-resolution STEM-ADF imaging was carried out on an aberration-corrected JEOL ARM200F, equipped with a cold field emission gun, operating at 60 kV.

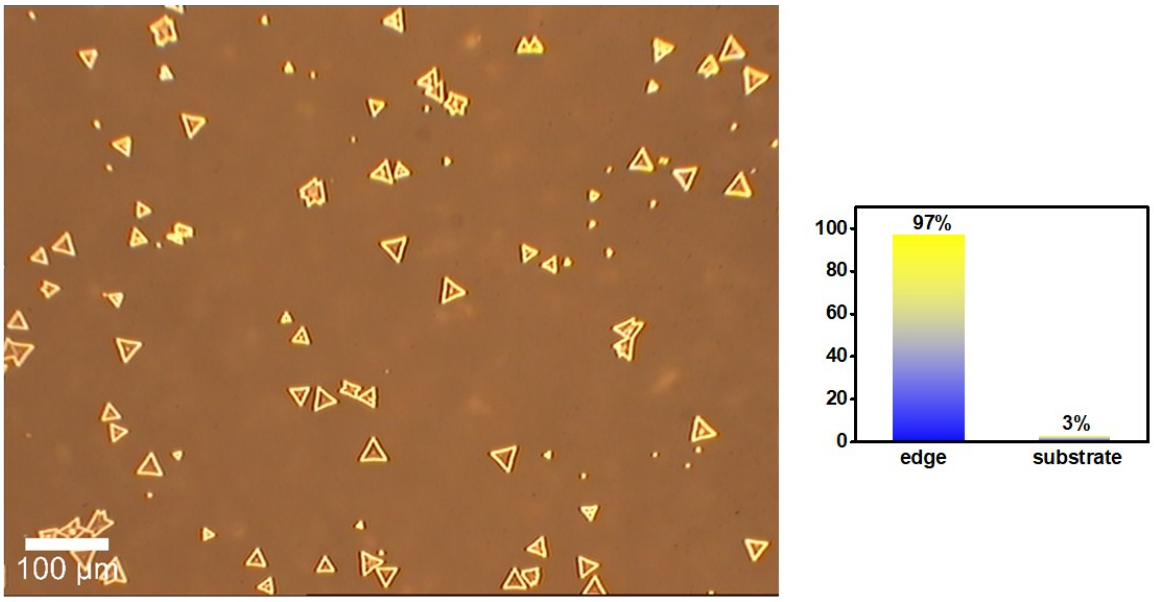

Figure S1. Optical microscopy images of the NbS_2/WS_2 heterostructure in large scale and the distribution of NbS_2 flakes on edge of WS_2 or substrate.

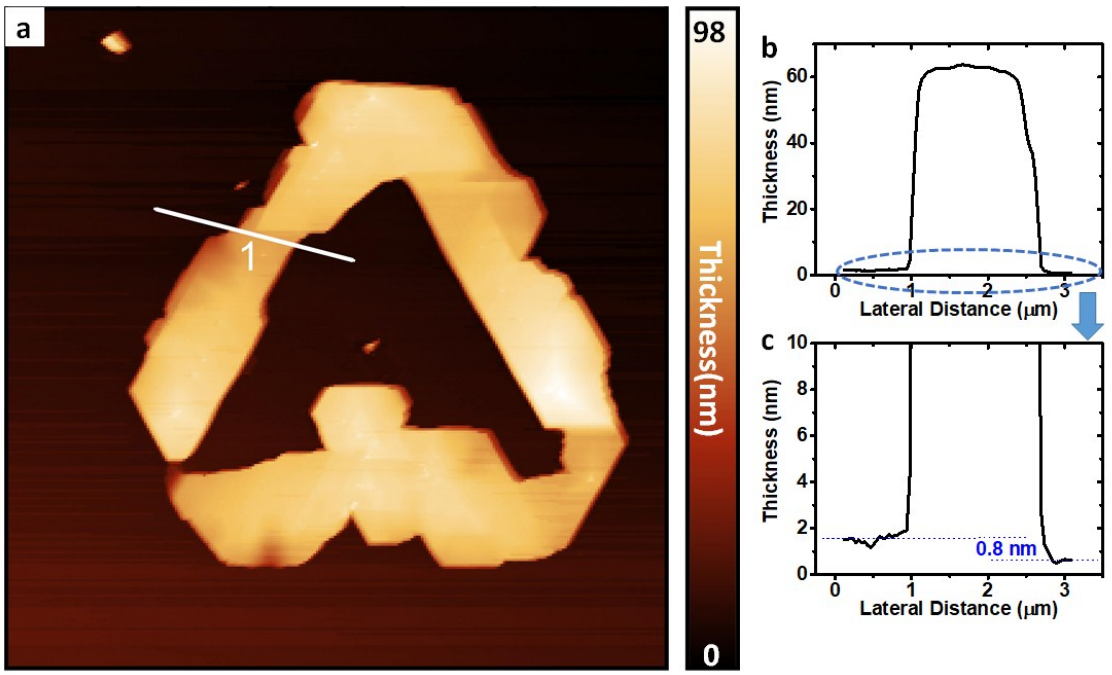

Figure S2. **a)** AFM height image of NbS_2/ WS_2 heterostructure; **b, c)** thickness of NbS_2 and WS_2.

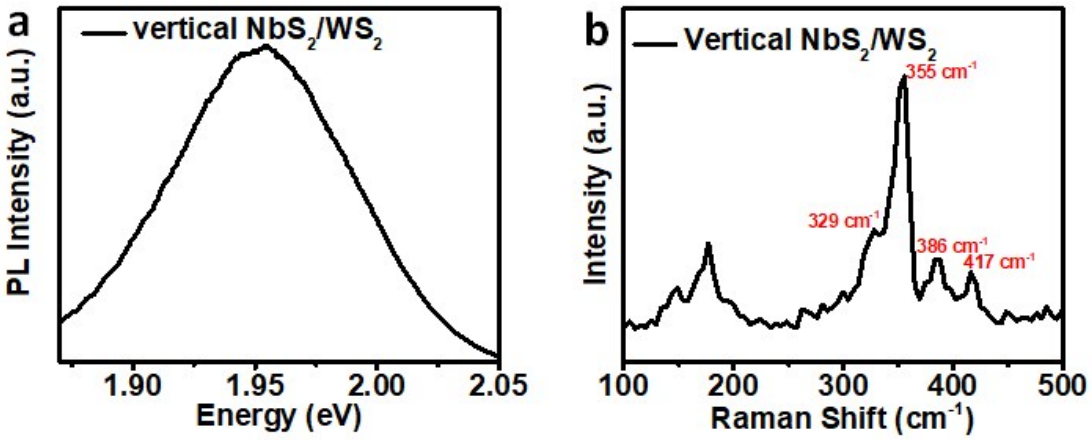

Figure S3. (a) PL spectrum of vertical NbS_2/WS_2 heterostructure and (b) its corresponding Raman curve.

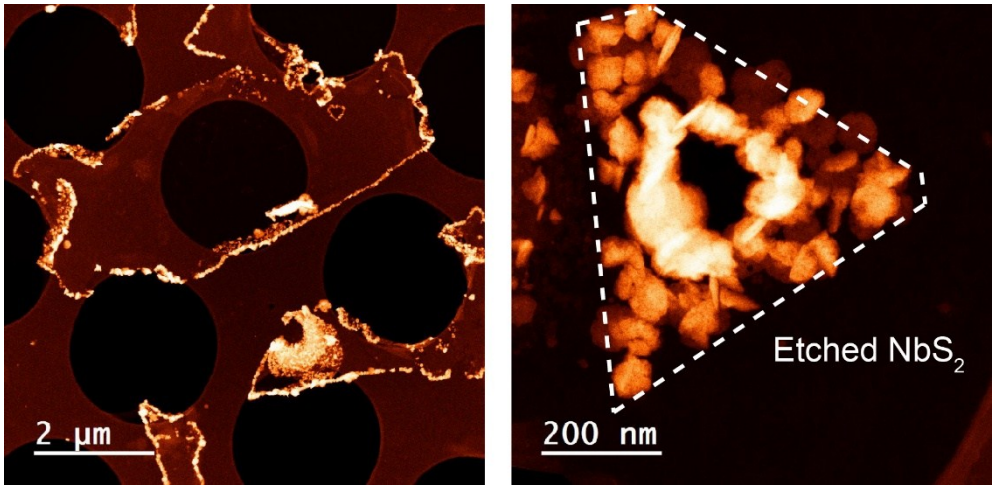

Figure S4. STEM-ADF images showing the morphology of the NbS_2/WS_2 heterostructures.

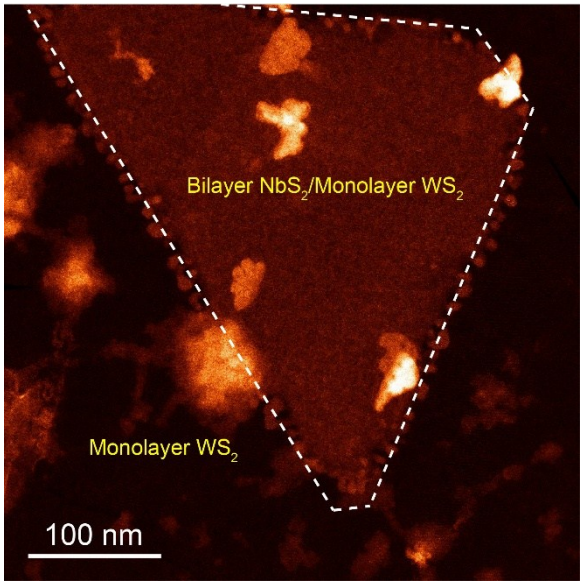

Figure S5. A STEM-ADF image depicting the morphology of the as-grown NbS_2/WS_2 heterostructure.

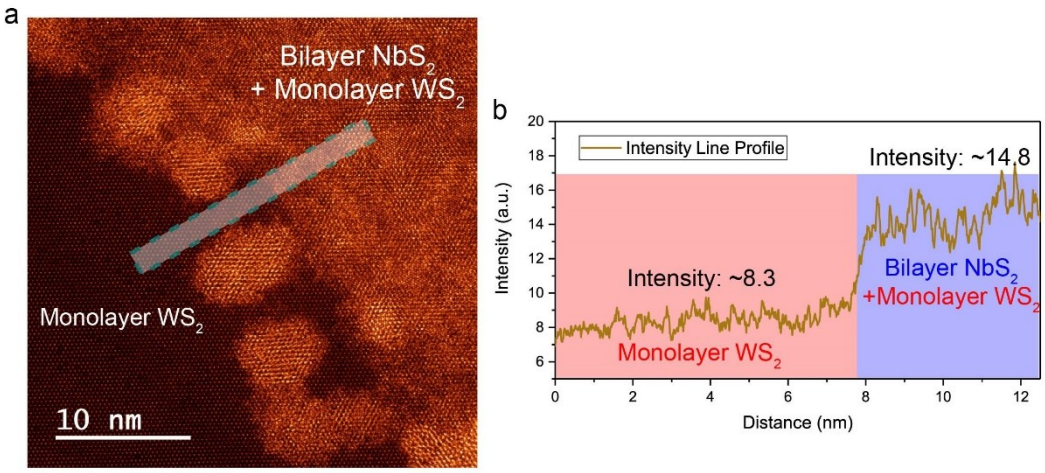

Figure S6. (a) An atomic-resolution STEM image showing the interface between monolayer WS_2 and vertical NbS_2/WS_2. (b) Intensity line profile of the white region in (a). According to the theoretical the image contrast between a monolayer WS_2 (W = 74; S = 16) to a bilayer NbS_2 (Nb = 41, S = 16) is about ~1.3. From the experimental image, the contrast of the monolayer WS_2 is around ~8.3, and the NbS_2/WS_2 region is about ~14.8 where the vacuum region is normalized to zero. The contrast ratio between the monolayer WS_2 to the as-grown NbS_2 is ~1.28, confirming the as-grown NbS_2 crystal is bilayer.

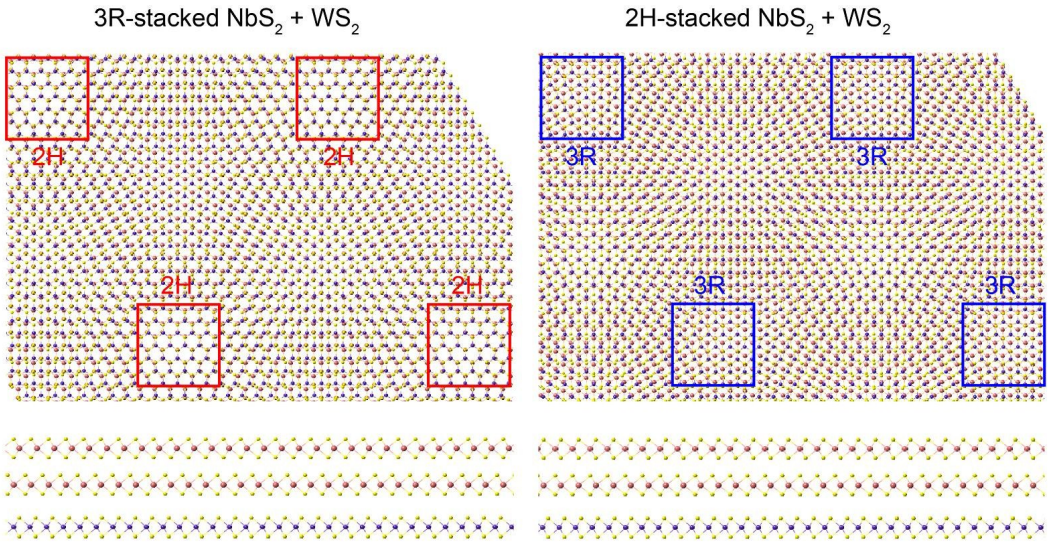

Figure S7. Atomic models showing the interlayer stacking registry evolution between 3R-stacked (left) and 2H-stacked NbS_2 with respect to the monolayer WS_2.